Spatial carrier-carrier correlations in strain-induced quantum dots

M. Braskén
Optoelectronics Laboratory, Helsinki University of Technology, FIN-02015 HUT, Finland

M. Lindberg
Department of Physics, Åbo Akademi University, FIN-20500 Turku, Finland

D. Sundholm
Department of Chemistry, University of Helsinki, FIN-00014 Helsinki, Finland

J. Olsen
Department of Chemistry, University of Aarhus, DK-8000 Aarhus, Denmark

(Received 6 November 2000; published 20 June 2001)

The electron-hole correlation effects on the energy levels and the wave functions of the electrons and holes in a strain-induced quantum dot containing one to ten carrier pairs have been studied using large-scale configuration-interaction calculations. The present calculations show the formation of excitons and biexcitons in the quantum dot. By increasing the number of carrier pairs, one observes a transition from a strongly correlated system to a quantum dot system for which the electron-electron and hole-hole correlations are dominated by exchange interaction and are relatively well described at the Hartree-Fock level, while for an accurate description of the electron-hole correlations configuration-interaction calculations are necessary. Ring-shaped carrier distributions emerge with increasing number of carrier pairs.

DOI: 10.1103/PhysRevB.64.035312 PACS number(s): 78.66.Fd, 85.35.Be, 71.35.−y, 71.45.Gm

I. INTRODUCTION

The possibility of observing and studying the photoluminescence from individual quantum dots (QD),[1–6] and thereby probing the details of their electronic structure, has made it increasingly relevant to include the electron-hole correlation effects in the calculation of the QD energy spectra. For an accurate treatment of the carrier-carrier correlations, the Hamiltonian of the QD system has to be diagonalized exactly. This is clearly impossible without some simplifying assumptions. Generally, two different types of approximations have been introduced to circumvent the size problem. For small QD systems ($\sim 1-5$ nm), an atomic cluster approach using many-body pseudopotential theory has been proposed.[7] Since the atomic cluster method is based on atomic one-particle basis sets, an accurate solution of the equations in the given one-particle basis is not possible for larger QD systems. For large, weakly confined QD systems ($\sim 10-100$ nm), the use of the effective-mass approximation is almost universal.[8–10] The electrons and the holes in the QD can then be treated as an interacting few-body system situated in an external confinement potential. Since the situation of a few confined carriers in the QD can be realized experimentally, it is of importance to solve the few-body problem exactly in order to judge the validity of the effective-mass approximation.

The Hartree-Fock (HF) model is the most common starting point for accurate solutions of the many-body Schrödinger equations. In the HF approximation, each particle moves independently of the other particles. Due to the antisymmetry requirement on the total wave function, the spatial correlation of electrons with parallel spins is partly considered even at the HF level. In his work we will use the definition of the word ''correlation'' put forward by Löwdin,[11] that the Coulomb correlation is those spatial correlations which are not considered at the HF level. The Coulomb correlation results in an increased probability of finding the electrons and the holes closer to each other, and a decreased probability of finding particles of equal charge very close to each other. In this work, the electron-hole correlation effects are considered by performing configuration-interaction calculations. The full configuration-interaction (FCI) model represents an exact solution of the effective-mass Schrödinger equation,[12] and it allows a systematic, numerical study of the correlations in the few-body quantum dot system. By comparing the HF and the CI results for a QD containing a different number of electron-hole pairs, the importance of the correlation effects on the total energy, on the chemical potential, and on the carrier distribution can be evaluated.

While the transition from a strongly correlated few-particle system to a system containing many electrons and holes has been studied extensively in bulk semiconductors and in quantum wells (QW),[13,14] considerably less effort has been devoted to how this transition occurs in zero-dimensional systems, such as QD's. In this paper, we present the results of FCI and of truncated, but extensive, CI calculations performed on a strain-induced QD (Ref. 15) containing one to ten electron-hole pairs. Besides the correlation energy, we investigate how the Coulomb interaction effects the distribution of the electrons and the holes within the QD. This is done by evaluating the pair-correlation function obtained from the many-particle wave function. In contrast to the QD electron-hole system studied in this work, the behavior of the pair-correlation function in QD's containing only electrons has been studied quite extensively at both the HF and at the exact level.[16–20]

In Sec. II the Hamiltonian and correlation functions are introduced. The numerical methods used for solving the many-particle equation are described in Sec. III, and the results for calculation on a QD containing one to ten pairs are given in Sec. IV.

II. THEORY

We describe the QD electron-hole system using the effective-mass model. In our QD system the strained QW lifts the heavy-hole (HH) and light-hole (LH) degeneracy at the γ point, separating the HH-LH bands by approximately 40 meV. Calculations show that the HH-LH coupling shifts the single-particle energies by only a few meV and that the HH component dominates for the lowest few hole states.[21,22] For the sake of simplicity, we therefore neglect the effects of the HH-LH mixing and only consider two bands in our Hamiltonian. The effective-mass Hamiltonian can then be written as

$$\begin{aligned}\hat{H}=&\int d\mathbf{x}\,\hat{\psi}_e^\dagger(\mathbf{x})\left(-\frac{\hbar^2\nabla^2}{2m_e}+U_{con}^e(\mathbf{x})\right)\hat{\psi}_e(\mathbf{x})\\&+\int d\mathbf{x}\,\hat{\psi}_h^\dagger(\mathbf{x})\left(-\frac{\hbar^2\nabla^2}{2m_h}+U_{con}^h(\mathbf{x})\right)\hat{\psi}_h(\mathbf{x})\\&+\frac{1}{2}\int d\mathbf{x}\int d\mathbf{y}\,V_{ee}(\mathbf{x}-\mathbf{y})\hat{\psi}_e^\dagger(\mathbf{x})\hat{\psi}_e^\dagger(\mathbf{y})\hat{\psi}_e(\mathbf{y})\hat{\psi}_e(\mathbf{x})\\&+\frac{1}{2}\int d\mathbf{x}\int d\mathbf{y}\,V_{hh}(\mathbf{x}-\mathbf{y})\hat{\psi}_h^\dagger(\mathbf{x})\hat{\psi}_h^\dagger(\mathbf{y})\hat{\psi}_h(\mathbf{y})\hat{\psi}_h(\mathbf{x})\\&-\int d\mathbf{x}\int d\mathbf{y}\,V_{eh}(\mathbf{x}-\mathbf{y})\hat{\psi}_e^\dagger(\mathbf{x})\hat{\psi}_h^\dagger(\mathbf{y})\hat{\psi}_h(\mathbf{y})\hat{\psi}_e(\mathbf{x}),\end{aligned}\quad(1)$$

where the integration over the coordinate $\mathbf{x}\equiv\mathbf{r},\sigma$ also includes the summation over the spin components, and $U_{con}^{e,h}$ are the electron and hole confinement potentials. The Coulomb interaction between the electrons and holes is assumed to be a pure Coulomb potential, but with a background dielectric constant. Since the electrons and the holes are distinct particles with different masses in our model, the electron and hole operators commute and there will appear no electron-hole exchange interaction term in Eq. (1).

The total correlation energy E_{corr} is defined as $E_{corr}=E_{FCI}-E_{HF}$, i.e., the difference between the FCI and the HF energy. Truncated CI calculations, such as all single and double CI (SDCI) calculations, consider in general more than 80% of the total correlation energy.[23] The energies of still larger CI expansions are even closer to the FCI results.

The magnitude of the correlation energy is one measure of the strength of the carrier-carrier correlation. A more direct way to detect the correlation effects is to study the spatial distribution of the carriers in the QD. By introducing the pair-correlation function, information about carrier-carrier correlations can be extracted from the *N*-particle wave function. The pair-correlation function is defined as

$$\rho_2(\mathbf{x}_1,\mathbf{x}_2)=N(N-1)\int d\mathbf{x}_3\cdots d\mathbf{x}_N|\Psi(\mathbf{x}_1,\mathbf{x}_2,\ldots,\mathbf{x}_N)|^2.\quad(2)$$

In Eq. (2), the quantity $\rho_2(\mathbf{x}_1,\mathbf{x}_2)$ gives the probability of simultaneously finding a particle at the spatial point $\mathbf{r}_1$ with spin σ_1, and another at $\mathbf{r}_2$ with spin σ_2. By fixing one coordinate of $\rho_2(\mathbf{x}_1,\mathbf{x}_2)$, one obtains for the one-pair case ($N_p=1$) $\rho_2(\mathbf{x}_1)=2|\Psi(\mathbf{x}_1,\mathbf{x}_2^0)|^2$, which gives the electron (or hole) probability distribution in an exciton. From the distribution function, $\rho_2(\mathbf{x}_1)$, one can deduce the probability of finding the other electrons and/or holes relative to the fixed one. For the QD systems containing many electron-hole pairs, the distribution function, $\rho_2(\mathbf{x}_1)$, provides information about the formation of multiexcitonic molecular states. By introducing a one-particle basis set $\{\varphi_i(\mathbf{x})\}$, Eq. (2) can be written as

$$\rho_2(\mathbf{x}_1,\mathbf{x}_2)=\sum_{ijkl}\phi_i(\mathbf{x}_1)\phi_j(\mathbf{x}_2)\phi_k^*(\mathbf{x}_1)\phi_l^*(\mathbf{x}_2)\rho_{ijkl},\quad(3)$$

where $\rho_{ijkl}=\langle\Psi|\hat{a}_i^\dagger\hat{a}_k^\dagger\hat{a}_l\hat{a}_j|\Psi\rangle$ is the two-particle density matrix.

Since we are mainly interested in the purely spatial correlations, the spatial two-particle correlation function can be obtained by summing over the spin degrees of freedom

$$\begin{aligned}\rho_2(\mathbf{r}_1,\mathbf{r}_2)=&\sum_{\sigma_1,\sigma_2}\rho_2(\mathbf{r}_1\sigma_1,\mathbf{r}_2\sigma_2)\\=&\rho_{\uparrow\uparrow}(\mathbf{r}_1,\mathbf{r}_2)+\rho_{\uparrow\downarrow}(\mathbf{r}_1,\mathbf{r}_2)+\rho_{\downarrow\uparrow}(\mathbf{r}_1,\mathbf{r}_2)\\&+\rho_{\downarrow\downarrow}(\mathbf{r}_1,\mathbf{r}_2),\end{aligned}\quad(4)$$

where $\rho_{\uparrow\uparrow}(\mathbf{r}_1,\mathbf{r}_2)$ is the contribution to ρ_2 arising from two particles at $\mathbf{r}_1$ and $\mathbf{r}_2$, both with spin $+\frac{1}{2}$, and similarly $\rho_{\uparrow\downarrow}(\mathbf{r}_1,\mathbf{r}_2)$ arises from two particles at $\mathbf{r}_1$ and $\mathbf{r}_2$ with spins $+\frac{1}{2}$ and $-\frac{1}{2}$, respectively. Each component yields the probability of finding two particles at certain positions in space and with a given spin configuration. By using the two-particle correlation function in Eq. (4), one can directly obtain the distribution function of the spatial separation between two particles as

$$\rho(R)=\int d\mathbf{r}_1\int d\mathbf{r}_2\,\delta(R-|\mathbf{r}_1-\mathbf{r}_2|)\rho_2(\mathbf{r}_1,\mathbf{r}_2).\quad(5)$$

To gain some insight into the structure of the two-particle correlation function, one can compare Eq. (4) to the corresponding HF expressions. In the HF approximation, when both coordinates refer to the same species (i.e., electrons or holes), the terms appearing in Eq. (4) reduce to

$$\rho_{\uparrow\uparrow}^{HF}(\mathbf{r}_1,\mathbf{r}_2)=\rho_\uparrow(\mathbf{r}_1)\rho_\uparrow(\mathbf{r}_2)-\rho_\uparrow(\mathbf{r}_2;\mathbf{r}_1)\rho_\uparrow(\mathbf{r}_1;\mathbf{r}_2)\quad(6)$$

for spin-up electrons or holes and an analogous expression when the two particles have down spins. For electrons or holes with antiparallel spins one gets

$$\rho_{\uparrow\downarrow}^{HF}(\mathbf{r}_1,\mathbf{r}_2)=\rho_\uparrow(\mathbf{r}_1)\rho_\downarrow(\mathbf{r}_2).\quad(7)$$

The corresponding correlation functions for electron-hole pairs are

$$\rho^{HF}_{\uparrow\uparrow}(\mathbf{r}_1,\mathbf{r}_2)=\rho_{\uparrow}(\mathbf{r}_1)\rho_{\uparrow}(\mathbf{r}_2), \tag{8}$$

$$\rho^{HF}_{\uparrow\downarrow}(\mathbf{r}_1,\mathbf{r}_2)=\rho_{\uparrow}(\mathbf{r}_1)\rho_{\downarrow}(\mathbf{r}_2). \tag{9}$$

The interpretation of the one-particle densities, such as $\rho_{\uparrow}(\mathbf{r}_1)$ and $\rho_{\downarrow}(\mathbf{r}_2)$, becomes more apparent when one expresses them in terms of a one-particle basis set $\{\varphi_i(\mathbf{x})\}$. In this case, one obtains

$$\rho_{\uparrow}(\mathbf{r}_1)=\sum_{i(\uparrow)}^{occ}\varphi_i^*(\mathbf{r}_1)\varphi_i(\mathbf{r}_1), \tag{10}$$

where the sum is over occupied spin-up orbitals. In Eq. (10), it can be seen that $\rho_{\uparrow}(\mathbf{r}_1)$ is simply the density of spin-up particles. An analogous expression can be obtained for spin-down particles. The density $\rho_{\uparrow}(\mathbf{r}_1;\mathbf{r}_2)$ appearing in Eq. (6) becomes

$$\rho_{\uparrow}(\mathbf{r}_1;\mathbf{r}_2)=\sum_{i(\uparrow)}^{occ}\varphi_i^*(\mathbf{r}_2)\varphi_i(\mathbf{r}_1), \tag{11}$$

which reduces to Eq. (10) when $\mathbf{r}_1=\mathbf{r}_2$. In the HF approximation, there is no correlation between the particles of opposite spin. The joint probability is simply the product of the two one-particle densities. This is clearly an approximation, as the Coulomb interaction correlates the motion of the particles. Also, the correlation function between electrons and holes always factorizes at the HF level, which is not the case at the correlated level of theory. This implies that a proper description of the spatial correlations requires that one must go beyond the single Slater determinant approximation.

To visualize the spatial carrier-carrier correlations, the two-particle correlation function with one fixed coordinate has been studied. The spatial two-particle correlation functions in Eq. (4) have been evaluated for the QD systems containing one to ten electron-hole pairs. The correlation contributions have been studied by comparing the correlation functions obtained at the HF and the CI levels of theory.

III. NUMERICAL CALCULATIONS

The QD sample modeled in our calculations is a strain-induced QD formed by the self-organizing growth of an InP island on top of a GaAs/$In_xGa_{1-x}As$ QW (Ref. 15) (Fig. 1). The carrier confinement potential $U^{e,h}_{con}(\mathbf{x})$ appearing in Eq. (1) can for this type of QD be calculated numerically, using only the material parameters and the sample structure as input. The details of how this is done has been presented earlier.[22] The material and structural parameters for the QD sample used in our calculations are given in Table I. The depth of the confinement potential caused by the InP stressor is ~70 meV for the electrons and ~30 meV for the holes.[24] The InP island and the confinement potentials are assumed to be cylindrically symmetric. The eigenstates can thus be labeled using the total angular momentum $L_z=L^e_z+L^h_z$, where the states $|L_z|=0,1,2,\ldots$ will be denoted $\Sigma,\Pi,\Delta,\ldots$, and by the total spins S^e and S^h. The superscripts e and h refer to electrons and holes, respectively.

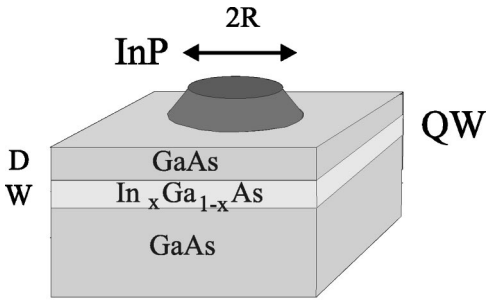

FIG. 1. Strain-induced QD sample. The material parameters and the dimensions of the QD sample used in our calculations are listed in Table I.

In the correlation calculations, the *N*-particle Hamiltonian of Eq. (1) is diagonalized in the configuration state function (CSF) basis. The FCI CSF basis consists of all the Slater determinants obtained by exciting the electrons and the holes from the HF reference to the unoccupied HF orbitals.[25] Since a FCI calculation represents the exact solution of the Schrödinger equation in the given one-particle basis set, the many-particle wave function will contain all the correlation effects. The first step in our computational approach is to solve the restricted HF equation.[26] The solution of the HF equation gives a set of optimized, occupied single-particle orbitals, and a complementary set of unoccupied ones. The CSF basis is then constructed from the set of occupied and unoccupied orbitals, and the corresponding Hamiltonian matrix is diagonalized.

Our FCI algorithm uses the direct CI approach, as implemented in the computer program LUCIA.[27,28] The direct CI method is based on the Davidson diagonalization algorithm,[28,29] which avoids storing and manipulating the entire Hamiltonian matrix and its eigenvectors. The factorial growth of the number of CSF's makes the FCI intractable for systems with many electrons and holes. To treat larger systems, one must use a truncated CSF basis. A systematic way of truncating the basis is to include all singly, doubly, triply, quadruply, (SDTQ), etc., excited Slater determinants in the CSF expansion. The all singles and doubles CI (SDCI) is, for instance, obtained by diagonalizing the Hamiltonian matrix in the CSF basis obtained by exciting at most two electrons, two holes, or one electron and one hole from the HF reference.

The single-particle wave functions for the electrons and the holes are expanded in an anisotropic Gaussian basis set of the form $x^{l_x}y^{l_y}z^{l_z}e^{-\alpha(x^2+y^2)}e^{-\beta z^2}$, where we denote the

TABLE I. The material parameters and the structure of the QD sample (see Fig. 1) used in our calculations. The values for the electron effective mass m_c and the parallel xy (to the QW) and perpendicular z components of the heavy-hole mass m_h are those in the QW. ϵ_r is the value of the relative dielectric constant in the QW.

D (nm)	$2R$ (nm)	W (nm)	x	ϵ_r	m_e	m_h^{xy}	m_h^z
5	80	7	0.1	13	$0.0665m_0$	$0.143m_0$	$0.34m_0$

functions with $l_x+l_y+l_z=0,1,2,\ldots$ by the letters $s,p,d,\ldots$. Since the confinement potentials are cylindrical symmetric, we use the same exponent α for the x and y functions. The strong quantum-well confinement allows us to reduce the size of our basis set by describing the z dependence by a few Gaussians with $l_z=0$. A basis set consisting of $4s4p3d$ basis functions has been used in our numerical calculations.[26] In this basis, we are able to perform FCI calculations on a QD containing up to four electron-hole pairs.[23] This results in a CSF basis consisting of about 68 million Slater determinants. The larger systems have been studied by performing truncated CI calculations, including all singly, doubly, triply, and quadruply excited determinants (SDTQCI). The validity of this approximation is justified by the fact that when comparing with the FCI calculations for the case of one to four pairs, one sees that the CI coefficient for higher than quadruple excitations are very small. The truncated CI calculations also correctly predict the experimentally observed rigid shell structure of the QD PL spectra.[23]

The diagonalization of the Hamiltonian matrix yields the eigenvectors of the few lowest eigenstates. The single-particle and two-particle density matrices and correlation functions are constructed from the eigenvectors. Hence, single-particle and two-particle expectation values can easily be evaluated for a specific eigenstate.

IV. RESULTS

A. Excitons

In Fig. 2 the correlation function $\rho_2(\mathbf{r}_e,\mathbf{r}_h^0)$ is plotted for the QD system with one electron-hole pair. The position of the hole ($\mathbf{r}_h^0$) has been fixed at $x_h=5$ nm, $y_h=5$ nm, and $z_h=0$. $\rho_2(\mathbf{r}_e,\mathbf{r}_h^0)$ is plotted in the $z_e=0$ plane, which defines the symmetry plane of the QW. The distance of the hole of ~ 7 nm from the center of the QD can be compared to the radius of the confinement potential, which is ~ 40 nm. This position for the fixed hole will be used throughout.

When fixing the hole coordinates of the exciton, and using Eqs. (8) and (9) in the conditional probability expression $P(\mathbf{r}_e;\mathbf{r}_h^0)=\rho_2^{HF}(\mathbf{r}_e,\mathbf{r}_h^0)/\rho_\uparrow(\mathbf{r}_h^0)$, one can see that the electron distribution is independent of the hole position at the HF level. In general, the two-particle correlation function does not factorize. Since the electron and the hole attract each other, one expects that the hole will drag the electron distribution along with it. As seen in Fig. 2, the probability distribution is not centered around the QD symmetry axis, as the HF result suggests. Instead, the electron follows the hole, clearly indicating the formation of a correlated electron-hole pair, i.e., an exciton. However, one can also see in Fig. 2 that the effect of the confinement potential is not negligible, as the electron stays in-between the hole and the QD center, which is the location of the potential minimum.

B. Biexcitons

For a QD system containing two electron-hole pairs ($N_p=2$), with both electrons and holes in the spin-singlet state, the HF calculations yield a centrally symmetric two-particle correlation function. Since there is no exchange interaction between particles with antiparallel spins, the two-particle correlation functions obtained at the HF level will show no spatial correlations.

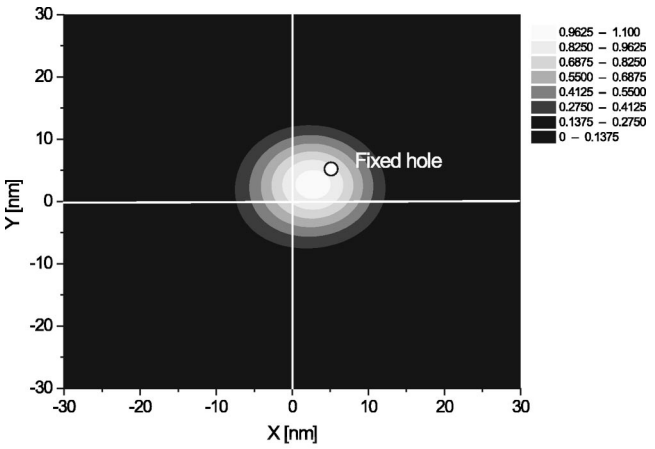

FIG. 2. Spatial two-particle correlation functions $\rho_2(\mathbf{r}_{e,h},\mathbf{r}_h^0)$ for one electron-hole pair ($N_p=1$). The QD symmetry axis defines the origin of the plot.

At the correlated level, one would expect that the system can either consist of two weakly interacting excitons or of a bound biexciton. Assuming that the two excitons are weakly interacting, then the two-particle correlation functions for the one and two exciton cases should not differ significantly. A stronger exciton-exciton interaction would result in the formation of biexcitons. A biexciton can be considered to be an excitonic analogue of the hydrogen molecule (H_2). As for H_2, the excitonic bond would show up in a higher probability of observing the electrons in the region between the two holes.

In Figs. 3(a) and 3(b), the correlation functions for the QD with two electron-hole pairs are illustrated. Figure 3(a) shows the electron-hole correlation $\rho_2(\mathbf{r}_e,\mathbf{r}_h^0)$, and Fig. 3(b) shows the hole-hole correlation $\rho_2(\mathbf{r}_h,\mathbf{r}_h^0)$. The spins of the two electrons and the two holes, respectively, are assumed to be antiparallel, each forming a spin-singlet state. The hole-hole correlation function in Fig. 3(b) shows that the fixed hole repels the other hole, pushing it to the opposite side of the QD center. What is more interesting, though, is that the electron-hole correlation function shows that the electron is most likely found in the region between the two holes. The position of the electrons is not purely a result of the confinement potential, since the pair-correlation function for the first excited $^1\Pi$ state shows that the preferred position for the electrons is between the two holes [see Figs. 4(a) and 4(b)]. These observations indicate the formation of a biexciton in the QD. The energy calculations show that the lowest $^1\Sigma$ of the biexciton has a positive binding energy, Δ_{XX}, of 2.0 meV relative to the energy of two noninteracting excitons. Since the exciton energies of the $\sigma_e\pi_h$ and the $\sigma_e\sigma_h$ complexes are -74.01 and -78.99 meV, respectively, the lowest $^1\Pi$ state is bounded by 1.55 meV as compared to the two noninteracting excitons.

Low-lying triplet states ($^3\Sigma$) can be constructed from two holes with parallel spin forming a triplet and from two elec-

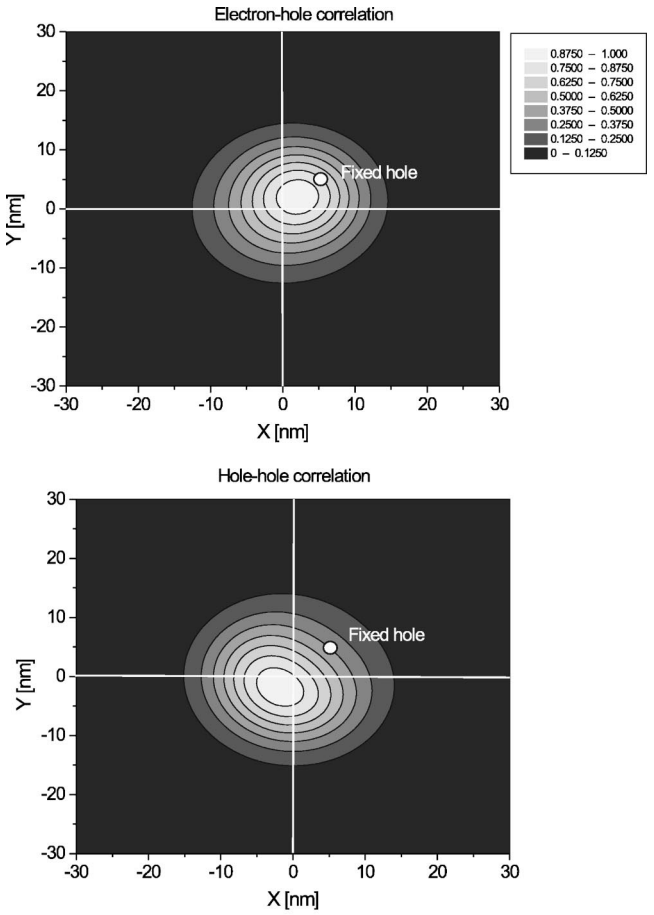

FIG. 3. Electron-hole (a) and the hole-hole (b) correlation functions for the $N_p=2$ system.

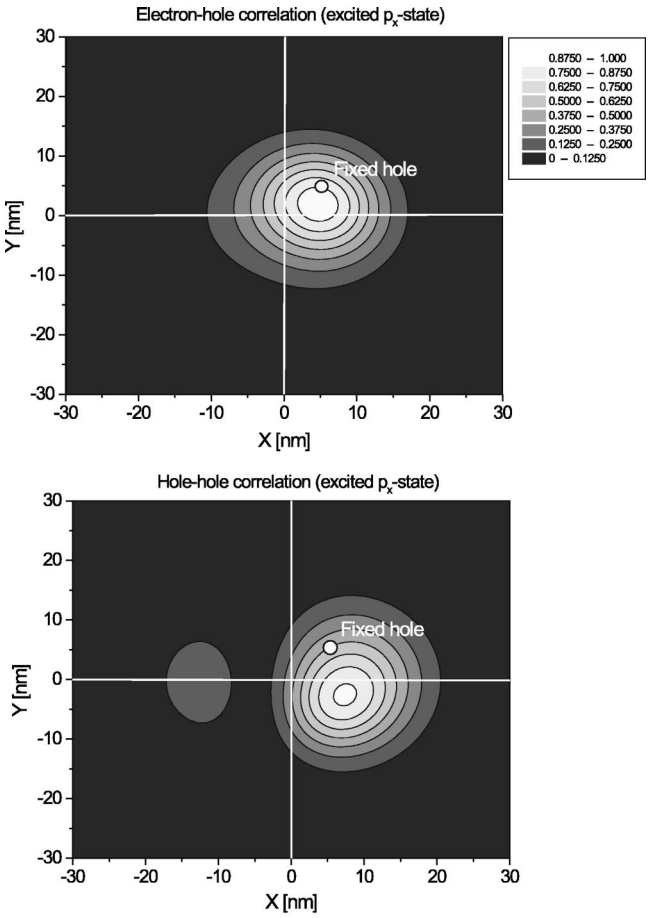

FIG. 4. Electron-hole (a) and the hole-hole (b) correlation functions for the lowest excited $^1\Pi$ state of the $N_p=2$ system.

trons with antiparallel spins forming a singlet. Alternatively, the two electrons form a triplet and the two holes a singlet. Of these two triplet states, the $^3\Sigma$ state with the two hole spins coupled to a triplet lies lower in energy. It is 9.4 meV above the $^1\Sigma$ ground state, while the second $^3\Sigma$ state is 15.3 meV above the ground state. This implies that the lowest $^3\Sigma$ state is not a bound biexciton. This situation is analogous to H_2, which is has a strongly bound singlet state, but a negative binding energy for the lowest triplet state. The lowest singlet $^1\Pi$ state which is also the first excited state of the biexciton lies 4.6 meV above the ground state.

The electron-hole correlation function for the $^1\Sigma$ and $^3\Sigma$ states are very similar. However, a significant difference is observed in the hole-hole correlation function (Fig. 5), clearly showing the effects of the exchange term. The exchange interaction carves out a minimum along a circle with the same radius as the distance between the fixed hole and the center of the QD. The other hole is forced partly inwards, but mostly outwards.

C. Multiexcitons

The interpretation of the correlation function $\rho_2(\mathbf{r}_1,\mathbf{r}_2)$ for QD systems containing more than two pairs is somewhat less obvious, since one cannot any longer identify the free coordinate with only one particle. What one sees instead is the sum distribution of the remaining electrons and holes. Since there are no strongly bound H_3, H_4, etc., molecules in nature to guide our intuition, it is not clear what will happen as more electron-hole pairs are added to the QD.

To see how the correlation energy changes as we add more pairs to the QD, the correlation energy (E_{corr}) is given

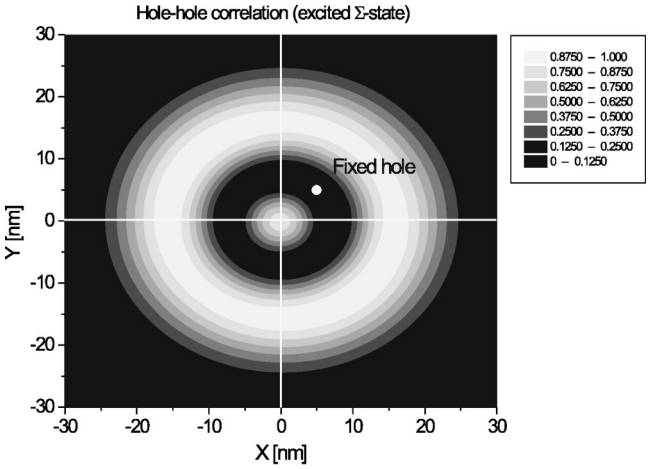

FIG. 5. Hole-hole correlation function for the first excited $^1\Sigma$ state of the $N_p=2$ system.

TABLE II. The correlation energy (in meV) of the ground state as a function of the number of electron-hole pairs N_p. For the QD systems with one to four electron-hole pairs, E_{CI} have been obtained at the FCI level, while for the QD systems containing more carrier pairs, E_{CI} have been calculated at the SDTQCI level.

N_p	E_{CI}	E_{HF}	E_{corr}	E_{corr}/N_p	$\mu_{CI}(N_p)$	$\mu_{HF}(N_p)$
1	−78.99	−77.76	−1.23	−1.23	−78.99	−77.76
2	−159.97	−155.53	−4.44	−2.22	−80.98	−77.76
3	−229.00	−218.40	−10.60	−3.53	−69.03	−62.87
4	−298.74	−290.59	−8.15	−4.04	−69.74	−72.19
5	−367.15	−354.43	−12.72	−2.54	−68.41	−63.84
6	−436.35	−427.55	−8.80	−1.47	−69.20	−73.11
7	−492.26	−479.77	−12.49	−1.78	−55.91	−52.23
8	−548.25	−539.43	−8.82	−1.10	−55.99	−59.66
9	−604.90	−596.30	−8.60	−0.96	−56.65	−56.87
10	−661.13	−653.34	−7.79	−0.78	−56.23	−57.04

in Table II as a function of the number of electron-hole pairs (N_p). As seen in Table II, the correlation energy as a function of N_p grows for QD systems containing up to three pairs and then the correlation energy starts to oscillate around −10 meV. This implies that the correlation energy per pair reaches a maximum for three pairs and then it starts to slowly decrease.[30,31]

The correlation energy is, however, only one indicator of the strength of the correlations. Figures 6(a) and 6(b) show the pair-correlation functions obtained at the FCI level for the QD containing three electron-hole pairs. Again the stationary hole pulls the electrons towards it and pushes the other holes to the opposite side of the QD. While the electron-hole pair-correlation function obtained at the HF level [Fig. 7(a)], $\rho_2^{HF}(\mathbf{r}_e,\mathbf{r}_h^0)$, is symmetric around the QD axis, the hole-hole correlation function, $\rho_2^{HF}(\mathbf{r}_h,\mathbf{r}_h^0)$, shows a displaced hole distribution [Fig. 7(b)]. This means that the significant part of the hole-hole correlation seen in Figs. 6(b) and 7(b) arises from the hole-hole exchange term, while configuration-interaction calculations are needed for obtaining the large spatial electron-hole correlation effects seen by comparing Figs. 6(a) and 7(a).

Since the correlation energy in Table II increases quadratically with the number of electron-hole pairs for the QD systems containing one to three pairs, it seems as if at least triexcitons are formed in the QD system. As seen in Figs. 6(a) and 6(b), the electrons prefer to be located between the fixed hole and the two remaining holes, which are pushed to the other side of the QD, forming a ''chemical'' bond. Since the pair-correlation functions in this case consist of several indistinguishable contributions, a thorough interpretation is nontrivial.

The calculation of the energy spectrum for one to four electron-hole pairs has been presented earlier.[23] The relative exciton energies, i.e., the stabilization energies, can be defined as

$$E_{stab}=E(N_p)-E(N_p-1)+E_X^{s,p,d}, \qquad (12)$$

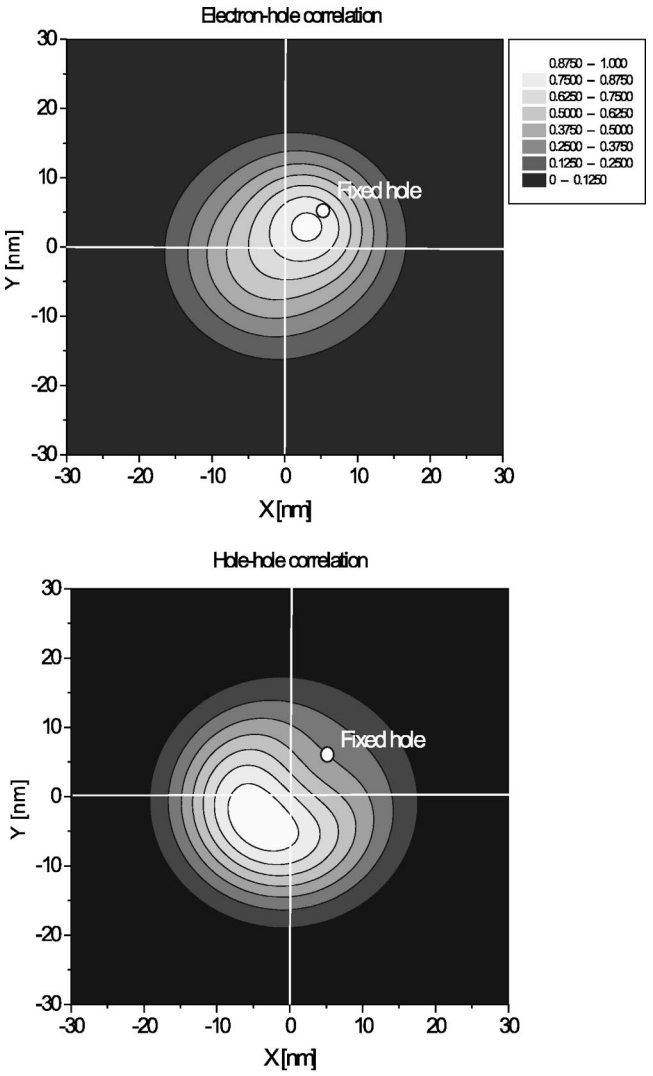

FIG. 6. Electron-hole (a) and the hole-hole (b) correlation functions for the $N_p=3$ system.

where $E(N_p)$ is the ground-state energy of the QD with N_p electron-hole pairs, and $E_X^{s,p,d}$ are the energies of the *s*, *p*, and *d* excitons, respectively. In Table III the exciton stabilization energies obtained from Eq. (12) are given. As seen in Table III, the ground states of all the studied QD systems are bound relative to the dissociation of the complex consisting of N_p electron-hole pairs into a multiexciton with N_p-1 electron-hole pairs and an exciton. Since we use a truncated CI expansion for $N_p>4$, the stabilization energy for the QD system with $N_p=5$ is somewhat smaller than for the others. The stabilization energy increases with an increasing number of electron-hole pairs in the dot. This suggests a relative strong interaction between the excitons and the formation of stable multiexciton complexes. Jacak, Hawrylak, and Wojs[32] suggested recently that the biexcitonic binding energy exceeds the binding energy of the larger excitonic complexes, implying that the QD containing many electrons and holes form a system of weakly interacting biexcitons. The present study shows that this is apparently not the case in our QD system.

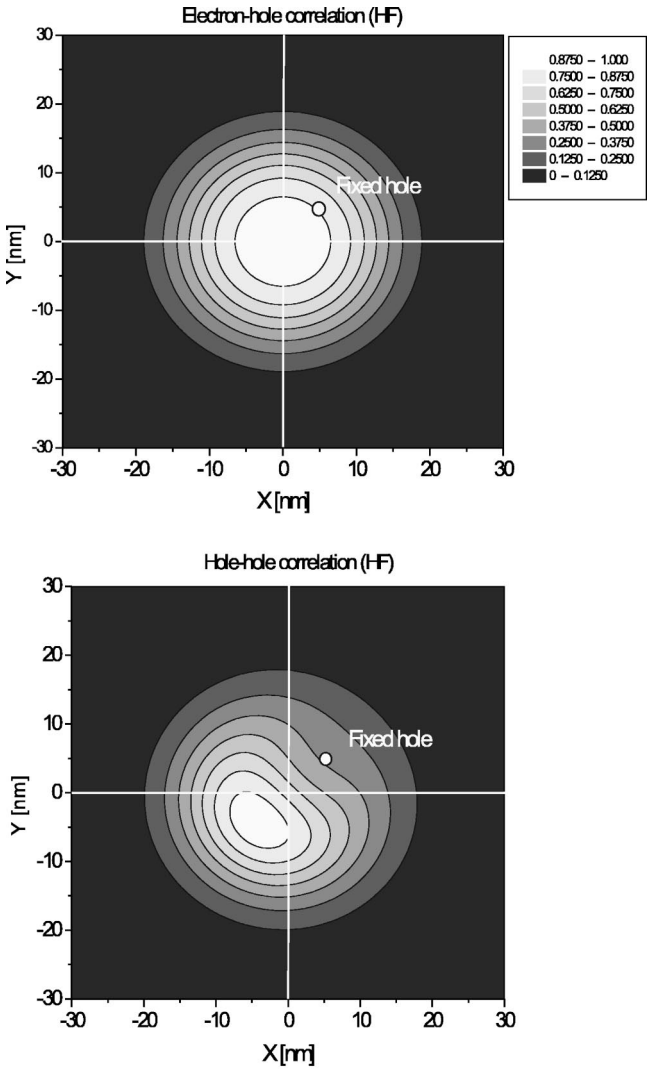

FIG. 7. Electron-hole and hole-hole correlation functions for $N_p=3$ calculated at the HF level.

TABLE III. The total energies of the multiexcitons and their stabilization energies (in meV) as a function of the number of electron-hole pairs, N_p.

N_p	$E(N_p)$	ΔE_{stab}	$E_X^{s,p,d}$
2	−159.97	−1.99	−78.99[a]
3	−229.00	−5.28	−63.75[b]
4	−298.74	−5.99	−63.75
5	−367.15	−4.66	−63.75
6	−436.35	−5.45	−63.75
7	−492.26	−7.56	−48.35[c]
8	−548.25	−7.64	−48.35
9	−604.90	−8.30	−48.35
10	−661.13	−7.88	−48.35

[a]The energy of the $\sigma(e)\sigma(h)$ exciton (E_X^s).
[b]The energy of the $\pi(e)\pi(h)$ exciton (E_X^p).
[c]The energy of the $\delta(e)\delta(h)$ exciton (E_X^d).

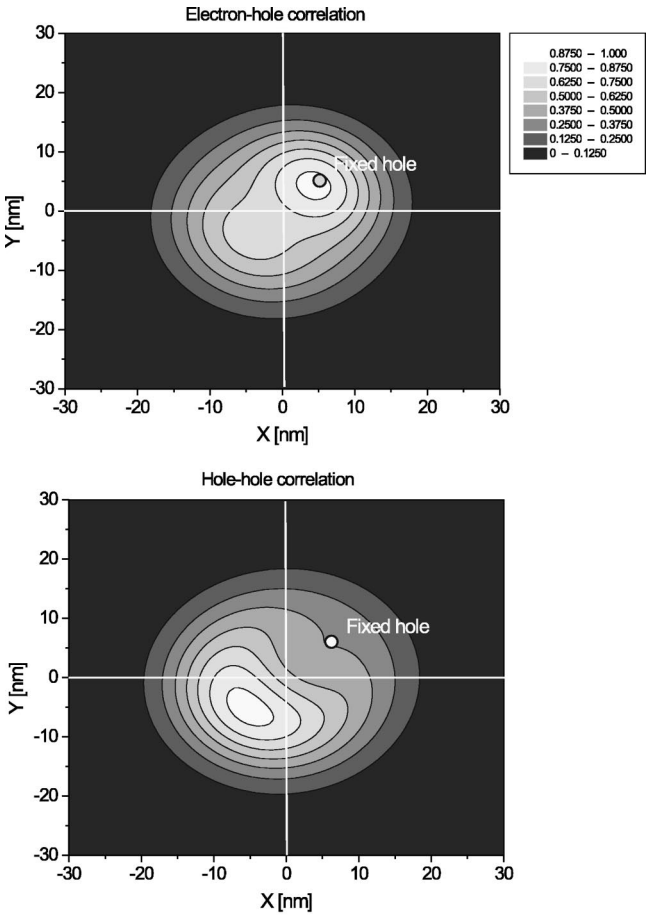

FIG. 8. Electron-hole (a) and the hole-hole (b) correlation functions for the $N_p=4$ system.

Figures 8(a) and 8(b) show the pair-correlation functions obtained at the FCI level for the QD containing four electron-hole pairs. As for the QD containing three electron-hole pairs, the fixed hole pushes the rest of the holes to the other side of the QD center, while most of the electrons are located around the fixed hole. However, now a significant part of the electrons are attracted by the hole distribution on the other side of the QD. The electrons seem to form a ''chemical'' bond between the fixed hole and the rest of the holes. This structure seems to be the first sign of the crescentlike shape of the hole-hole correlation functions and the ring-shaped electron-electron correlation functions obtained for the QD systems containing five to ten electron-hole pairs.

As we add more pairs to the QD, the hole distribution starts to spread out due to the Coulomb repulsion between the holes. A similar spread is also seen in the electron distribution, since they follow the holes. For six pairs, the hole distribution spreads out into a crescent shape. A crescent that almost forms a ring for ten pairs (Fig. 9). By comparing the hole-hole correlation function obtained at the HF level to results of the SDTQCI calculations, the same broad features can be seen at both levels of theory (Fig. 10). The only major difference is the more pronounced Coulomb hole seen around the fixed hole in the SDTQCI results.

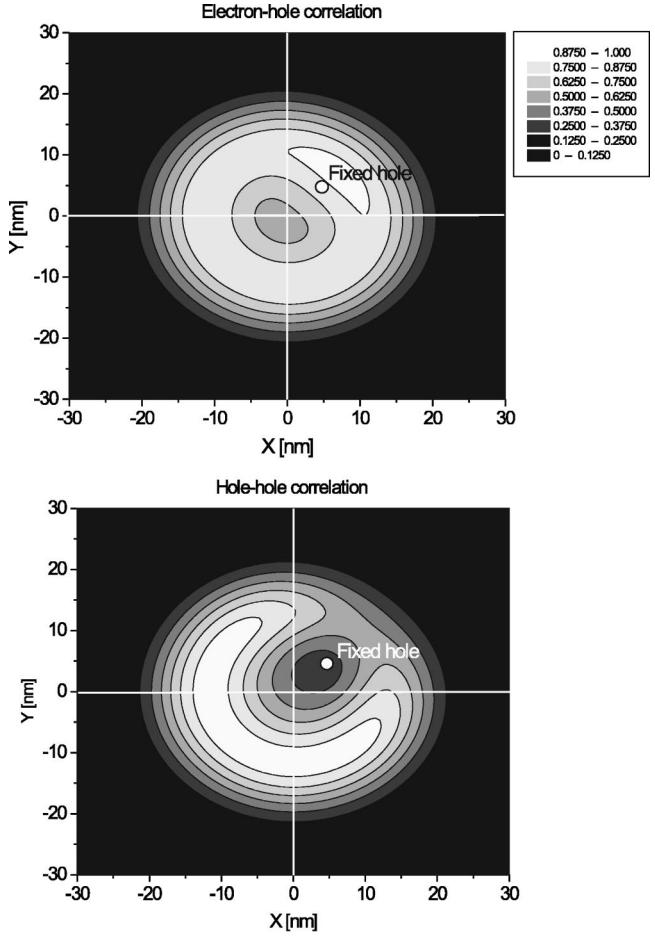

FIG. 9. Electron-hole (a) and the hole-hole (b) correlation functions for the $N_p=10$ system.

D. Average carrier separation

An interesting possibility that arises when observing the ring-shaped structure formed by the electron-hole system is the formation of a crystalline structure similar to the Wigner crystal suggested to exist in QD's confining only electrons.[33] A crystalline structure would show up as distinct peaks in the carrier separation distribution $\rho(R)$, introduced in Eq. (5), for certain carrier separations R. For an exciton, the maximum of $\rho(R)$ gives the exciton Bohr radius R_X, which for our QD system is $R_X=7.0$ nm. As more pairs are added to the QD, the carrier separation distribution broadens. As seen in Fig. 11, the more carrier pairs in the QD system, the closer the HF result comes to the CI results. The monotonous broadening of both the electron-hole and hole-hole (not shown) distance distribution implies that there are no preferred distances between the carriers inside the ring, suggesting that no crystalline structure is formed in our QD system.

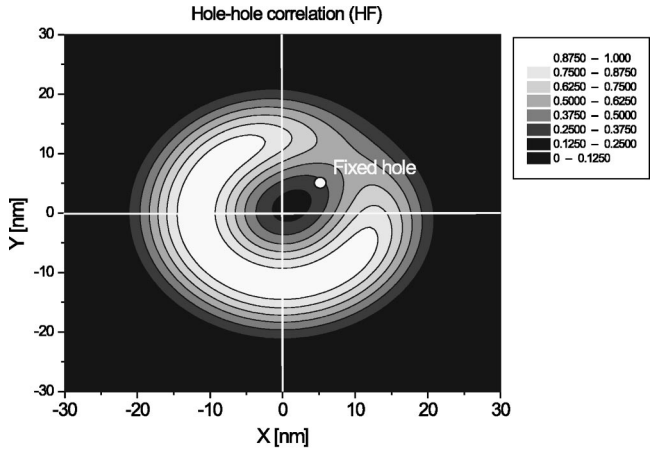

FIG. 10. Hole-hole correlation function for the $N_p=10$ case calculated at the HF level.

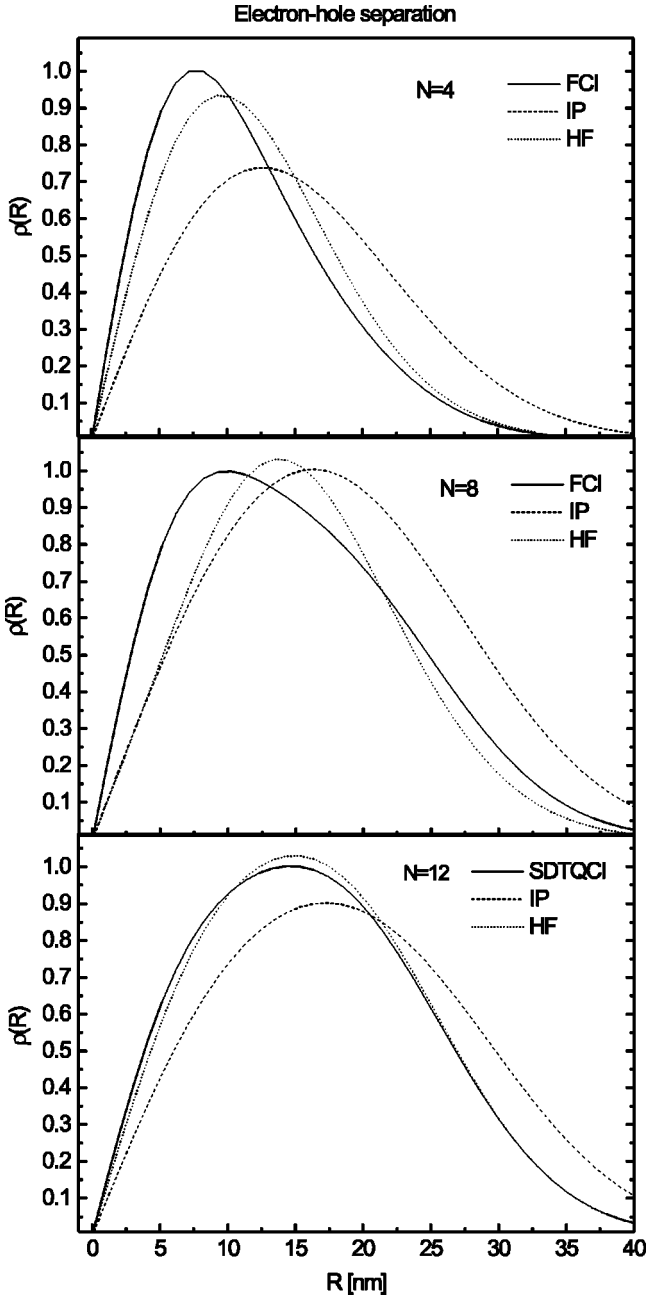

FIG. 11. Distance distribution function for the $N_p=2$, $N_p=4$, and $N_p=6$ systems.

V. SUMMARY

The electron-hole correlation effects for a strained-induced QD consisting of an InP island on top of a $GaAs/In_xGa_{-x}As$ QW have been studied by performing extensive CI calculations. The calculations show the importance of the carrier-carrier correlations. For one and two electron-hole pairs the HF solutions factorize, which implies that the spatial correlation is only introduced at the correlated level. The spatial electron-electron and the hole-hole correlations for QD's containing many electron-hole pairs is dominated by the exchange interaction, which is obtained already at the HF level. However, to consider the electron-hole correlation effects the calculations have to be performed at a correlated level of theory. The spatial correlation functions show the formation of excitons and biexcitons, while for QD systems containing many electron-hole pairs the interpretation of the correlation functions is nontrivial. The binding of two excitons to a biexciton can be observed in the correlation function as an increased probability of finding the two electrons between the holes analogously to the formation of the chemical bond in molecular systems. For the QD system containing six electron-hole pairs, the correlation functions become ring shaped, while when further pairs are added to the QD, the correlation functions are ring shaped. The calculated stabilization energies suggest the formation of multiexciton complexes.

ACKNOWLEDGMENTS

We thank Professor P. Pyykkö and The Academy of Finland for generous support. We acknowledge the support from the European Research Training Network on ''Molecular properties and Molecular Materials'' (MOLPROP), Contract No. HPRN-2000-00013.

[1] M. Bayer, O. Stern, P. Hawrylak, S. Fafard, and A. Forchel, Nature (London) **405**, 923 (2000).
[2] R.J. Warburton, C. Schäflein, D. Haft, F. Bickel, A. Lorke, K. Karrai, J.M. Garcia, W. Schoenfeld, and P.M. Petroff, Nature (London) **405**, 926 (2000).
[3] P. Michler, A. Imamoglu, M.D. Mason, P.J. Carson, G.F. Strouse, and S.K. Buratto, Nature (London) **406**, 6799 (2000).
[4] M. Bayer, T. Gutbrod, A. Forchel, V.D. Kulakovskii, A. Gorbunov, M. Michel, R. Steffen, and K.H. Wang, Phys. Rev. B **58**, 4740 (1998).
[5] L. Landin, M.-E. Pistol, C. Pryor, M. Persson, L. Samuelsson, and M. Miller, Phys. Rev. B **60**, 16 640 (1999).
[6] E. Dekel, D. Gershoni, E. Ehrenfreund, J.M. Garcia, and P.M. Petroff, Phys. Rev. B **61**, 11 009 (2000).
[7] A. Franceschetti, H. Fu, L.W. Wang, and A. Zunger, Phys. Rev. B **60**, 1819 (1998).
[8] G. Bryant, Phys. Rev. B **37**, 8763 (1988).
[9] E. Dekel, D. Gershoni, E. Ehrenfreund, D. Spektor, J.M. Garcia, and P. M. Petroff, Phys. Rev. Lett. **80**, 4991 (1998).
[10] P. Hawrylak, Phys. Rev. B **60**, 5597 (1999).
[11] P.-O. Löwdin, Adv. Chem. Phys. **2**, 207 (1959).
[12] In a real calculation one has to use a finite basis set, which makes the solution approximate. However, the error introduced by the finite basis can be estimated by checking the basis set convergence.
[13] G. Bartels, A. Stahl, V.M. Axt, B. Haase, U. Neukirch, and J. Gutowski, Phys. Rev. Lett. **81**, 5880 (1998).
[14] B. Haase, U. Neukirch, J. Gutowski, G. Bartels, A. Stahl, V.M. Axt, J. Nürnberger, and W. Faschinger, Phys. Rev. B **59**, R7805 (1999).
[15] H. Lipsanen, M. Sopanen, and J. Ahopelto, Phys. Rev. B **51**, 13 868 (1995).
[16] P.A. Maksym, Physica B **184**, 385 (1993).
[17] P.A. Maksym, Phys. Rev. B **53**, 10 871 (1995).
[18] C. Yannouleas and U. Landman, Phys. Rev. Lett. **82**, 5325 (1999).
[19] C. Yannouleas and U. Landman, Phys. Rev. B **61**, 15 895 (2000).
[20] C. Yannouleas and U. Landman, Phys. Rev. Lett. **85**, 1726 (2000).
[21] M. Braskén, M. Lindberg, and J. Tulkki, Phys. Rev. B **55**, 9275 (1997).
[22] J. Tulkki and A. Heinämäki, Phys. Rev. B **52**, 8239 (1995).
[23] M. Braskén, M. Lindberg, D. Sundholm, and J. Olsen, Phys. Rev. B **61**, 7652 (2000).
[24] The form of the confinement potential resembles that of truncated 2D parabolic potential, with a typical width of *D*.
[25] R. McWeeny, *Methods of Molecular Quantum Mechanics* (Academic Press, London, 1992).
[26] M. Braskén, M. Lindberg, D. Sundholm, and J. Olsen, in *Atoms, Molecules, and Quantum Dots in Laser Fields: Fundamental Processes*, Pisa 2000, edited by N. Bloembergen, N. Rahman, and A. Rizzo, Conf. Proc. Vol. 71 (Societa Italiana di Fisica, Bologna, 2001), p. 315.
[27] LUCIA is a direct CI program written by J. Olsen (unpublished).
[28] J. Olsen, P. Jørgensen, and J. Simons, Chem. Phys. Lett. **169**, 463 (1990).
[29] E. Davidson, J. Comput. Phys. **17**, 87 (1975).
[30] A. Wojs and P. Hawrylak, Phys. Rev. B **55**, 13 066 (1997).
[31] Since we use a truncated CI expansion for $N_p>4$ the obtained correlation energy will be somewhat smaller than the FCI value. For the $N_p=4$ case, the SDTQ truncation introduces an 0.6-meV reduction in E_{corr} as compared to the FCI result.
[32] L. Jacak, P. Hawrylak, and A. Wojs, *Quantum Dots* (Springer, Berlin, 1998).
[33] P.A. Maksym, H. Imamura, G.P. Mallon, and H. Aoki, J. Phys.: Condens. Matter **12**, R299 (2000).